ELSEVIER

Journal of Organometallic Chemistry 504 (1995) 15–26

Journal of Organometallic Chemistry

# H/D exchange via reversible pyridine ortho-metallation, and competition between C–H oxidative addition and CO coordination in hydrido–carbonyl triangular rhenium clusters: a $^1$H-NMR investigation. X-ray crystal structure of the anion $[Re_3(\mu\text{-}H)_2(CO)_{11}(Py)]^-$

T. Beringhelli [a], L. Carlucci [b], G. D'Alfonso [a,*], G. Ciani [b,*], D.M. Proserpio [b]

[a] *Dipartimento di Chimica Inorganica, Metallorganica e Analitica and Centro C.N.R., Via Venezian 21, Milano, Italy*
[b] *Dipartimento di Chimica Strutturale e Stereochimica Inorganica and Centro C.N.R., Via Venezian 21, Milano, Italy*

Received 11 January 1995; in revised form 24 March 1995

**Abstract**

The triangular cluster anion $[Re_3(\mu\text{-}H)_3(\mu\text{-}NC_5H_4)(CO)_{10}]^-$ (**2**), containing an ortho-metallated pyridine bridging a cluster edge, undergoes in acetone solution a selective H/D exchange between the basal hydridic site and the $\alpha$-position of the ortho-metallated pyridine, with $k = 1.9(1) \times 10^{-6}$ s$^{-1}$, at room temperature. The process was studied by NMR on the partially deuterated derivative $[Re_3(\mu\text{-}H)_2(\mu\text{-}D)(\mu\text{-}NC_5D_4)(CO)_{10}]^-$ and an equilibrium isotope effect was observed, the equilibrium concentration of the isotopomer containing C-bound deuterium being about double that of the isotopomer containing Re-bound deuterium. In pyridine-$d_5$ solutions, in contrast, the preferential deuteration of the hydrides bridging the lateral edges of $[Re_3(\mu\text{-}H)_3(\mu\text{-}NC_5H_4)(CO)_{10}]^-$ was observed, with a rate about half that of the deuteration of the ortho-metallated pyridine ($k = 2.9(1) \times 10^{-5}$ s$^{-1}$ at 302 K for the latter process). The H/D exchange processes in both solvents have been rationalized as arising from the reversible reductive elimination of the ortho-metallated pyridine. The different behavior in the two solvents is discussed. In the presence of CO, the anion **2** gave $[Re_3(\mu\text{-}H)_2(CO)_{12}]^-$ (**4**, $t_{1/2} \approx 48$ h) in acetone solution, while in pyridine it gave the novel anion $[Re_3(\mu\text{-}H)_2(CO)_{11}(Py)]^-$ (**3**). In py-$d_5$, under CO, the resonances of the ortho-metallated pyridine of **2** decreased at the same rate as in the absence of CO. The competition ratio $r$ between CO coordination and pyridine ortho-metallation on the intermediate generated by C–H reductive elimination has been estimated as 0.45(15). The reaction of $[Re_3(\mu\text{-}H)_4(CO)_{10}]^-$ (**1**) with CO in pyridine follows two parallel paths, affording both compounds **3** and **2**, the latter, in turn, converting into **3** at a slower rate. The rate of disappearance of **1** was the same as that measured in the absence of CO ($k = 2.1(2) \times 10^{-4}$ s$^{-1}$ at 302 K) and the value of the competition ratio $r$ between the two pathways leading to **3** and **2**, respectively, was found to be 0.5(1). Under high $H_2$ pressure, **2** slowly transforms back into the unsaturated parent anion **1**, showing the complete reversibility of the ortho-metallation reaction. The structure of the anion $[Re_3(\mu\text{-}H)_2(CO)_{11}(Py)]^-$ (**3**), as $[NEt_4]^+$ salt, has been investigated by X-ray analysis. The crystals are monoclinic, space group $P2_1/c$, with $a = 14.327(3)$, $b = 12.310(2)$, $c = 17.437(3)$ Å, $\beta = 91.67(2)°$ and $Z = 4$. The refinements, performed by full-matrix least-squares on the basis of 2064 significant [$I > 2\sigma(I)$] reflections, gave final agreement indices $R$ and w$R^2$ of 0.0397 and 0.0835, respectively. The anion contains an isosceles triangle of rhenium atoms, with one shorter edge [3.025(1) Å], and two longer hydrogen-bridged edges [3.202(1) and 3.209(1) Å]; it bears eleven terminal CO groups and an N-bonded pyridine molecule [Re–N 2.21(2) Å].

*Keywords:* Rhenium; Pyridine; Metal clusters; Ortho-metallation

## 1. Introduction

One of the main interests in the chemistry of molecular clusters relies on their providing reliable models of the polycentric interactions of organic molecules on metallic surfaces [1]. In particular, examples of reversible activation of the C–H bonds of ligands coordinated on metal clusters have been reported [2]. Such reactions require coordinatively unsaturated metal centres and are therefore affected by the presence of ligands (such as CO) that can "poison" the active metallic site, by coordination on it. In this work the reversible oxidative addition of the C–H bond of a pyridine

* Corresponding authors.

Elsevier Science S.A.
*SSDI* 0022-328X(95)05602-5

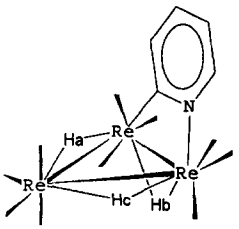


Scheme 1.

molecule bound to a triangular rhenium cluster and the influence of CO on this reactivity have been studied.

We have recently reported [3] that the reaction of the unsaturated anion $[Re_3(\mu\text{-}H)_4(CO)_{10}]^-$ (**1**, 46 valence electrons) with pyridine (Eq. (1)) gives a product $[Re_3(\mu\text{-}H)_3(\mu\text{-}NC_5H_4)(CO)_{10}]^-$ (**2**, Scheme 1) containing an ortho-metallated pyridine molecule bridging a cluster edge.

$$[Re_3(\mu\text{-}H)_4(CO)_{10}]^- + Py \rightarrow [Re_3(\mu\text{-}H)_3(\mu\text{-}NC_5H_4)(CO)_{10}]^- + H_2 \quad (1)$$

The reaction of **1** with pyridine is different with respect to that occurring with other two-electron donor molecules L (L = CO [4], $PR_3$ [5] or MeCN), where the substitution of two L ligands for two hydrides was observed (Eq. (2)).

$$[Re_3(\mu\text{-}H)_4(CO)_{10}]^- + 2L \rightarrow [Re_3(\mu\text{-}H)_2L_2(CO)_{10}]^- + H_2 \quad (2)$$

The initial reaction steps are probably the same in both cases: addition of the donor molecule on the unsaturated cluster **1**, to give a 48 valence electrons adduct **I1** unstable toward $H_2$ reductive elimination (Scheme 2). This produces an intermediate **I2** containing a coordinatively and electronically unsaturated rhenium centre, which then can either add a second L ligand, or undergo the oxidative addition of the $C_\alpha$–H bond, when L = pyridine.

The results reported here have led to a better insight into the above described pathway. H/D exchange processes in different isotopomers of the anion **2** have been investigated in various conditions and shown to arise from the reversibility of the ortho-metallation reaction, to give an intermediate species **I2** similar to that formed by $H_2$ reductive elimination from **I1** in Scheme 2. The reactions of the anions **1** and **2** with CO in pyridine have been also studied by NMR and the results have been analyzed in terms of the competition between C–H oxidative addition and CO coordination on the intermediate **I2**. These reactions led to the novel cluster anion $[Re_3(\mu\text{-}H)_2(CO)_{11}(Py)]^-$, whose structure has been determined by X-ray single crystal analysis.

## 2. Results and discussion

### 2.1. The H / D exchange

The anion **2** exhibits three hydridic resonances at $\delta$ −12.26, −13.45, and −15.05 ppm, in acetone solution, which have been assigned to $H_b$, $H_c$ and $H_a$, respectively [3]. The reaction of the anion **1** with deuterated pyridine (py-$d_5$) has been shown [3] to give the isotopomer $[Re_3(\mu\text{-}H)_2(\mu\text{-}D)(\mu\text{-}NC_5D_4)(CO)_{10}]^-$, (**2b**). The presence of a deuteride on the cluster demonstrates that the metallation reaction occurs through a real oxidative addition mechanism [6]. The deuterium atom is equally distributed on the two lateral edges of the triangle (sites *a* and *c* of Scheme 1), as demonstrated by the 1:0.5:0.5 integration ratio of the hydridic resonances. This even distribution arises from a fluxional process [3] scrambling the deuterium atom, which is supposed to be initially located only in site *a*, between the sites *a* and *c*. The process is quite fast ($k$ slightly lower than 1 $s^{-1}$ at room temperature), even if slow on the NMR time scale.

On standing in py-$d_5$ all the hydridic resonances of **2b** lost intensity (Fig. 1), and the ratio between the resonance of $H_b$ and those of the other two hydrides slowly increased to about 0.6 after 5 h (when the reagent **1** was completely consumed) and to about 0.7

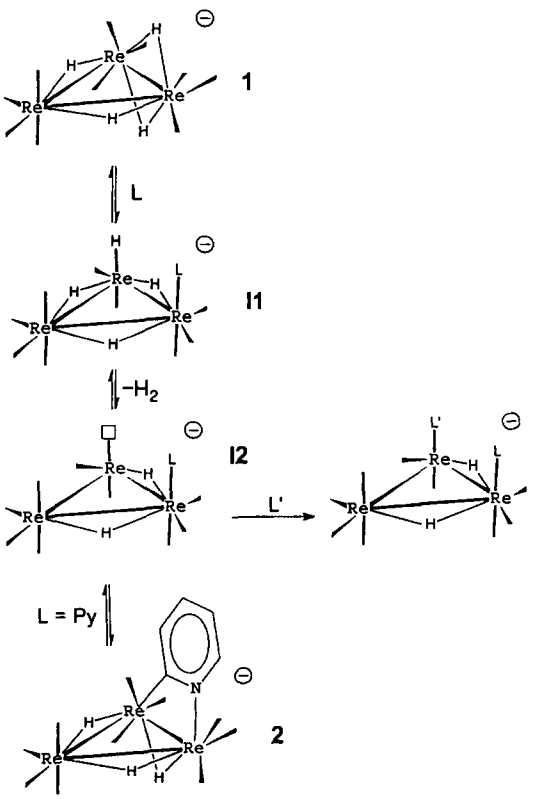


Scheme 2.

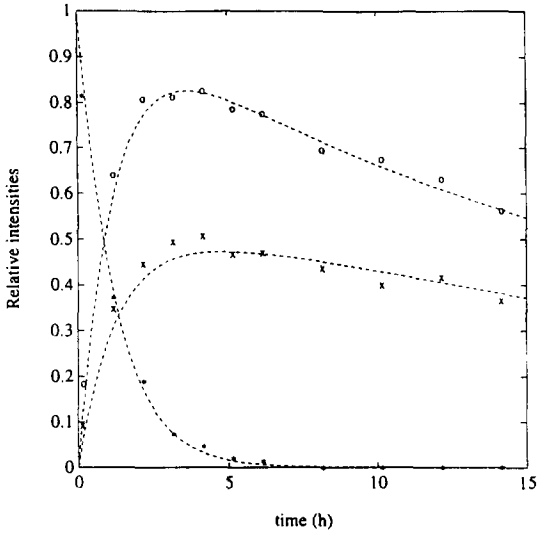


Fig. 1. Time course of the intensities of the resonances of **1** (*) and **2** (○, $H_b$; ×, $H_a$) during the reaction of **1** in py-$d_5$ at 302 K. The low field resonance of **1** was used and divided by 2, being due to 2 equivalent hydrides.

after one night. A $^2$H-NMR spectrum of a sample of **2** kept in py-$d_5$ for several days has confirmed that the disappearance of the protonic resonances is due to H/D exchange and not to decomposition of **2** [7].

Two experiments were performed to investigate the mechanism of the H/D exchange process.

In the first experiment a sample of $[Re_3(\mu\text{-}H)_2(\mu\text{-}D)(\mu\text{-}NC_5D_4)(CO)_{10}]^-$ (**2b**, $NEt_4^+$ salt) was dissolved in deuterated acetone, at room temperature (ca. 293 K) and spectra were acquired at different times. As shown in Fig. 2, a clean transfer of H atoms occurred from the hydridic site $H_b$ ($\delta$ −12.26) to the carbon atom in the $\alpha$ position of the ortho-metallated pyridine ($\delta$ 8.25).

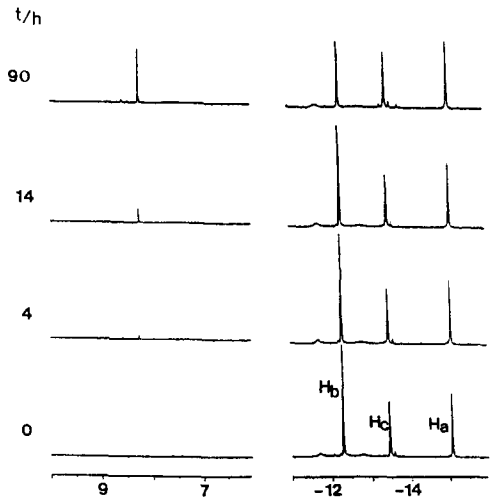


Fig. 2. Hydridic and pyridinic regions of the 200.13 MHz NMR spectra of $[Re_3(\mu\text{-}H)_2(\mu\text{-}D)(\mu\text{-}NC_5D_4)(CO)_{10}]^-$ (**2b**) in acetone-$d_6$ solution at different times.

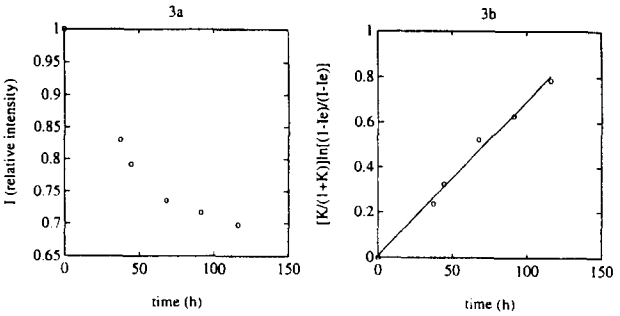


Fig. 3. (a) Time course of the intensity $I$ of the resonance at $\delta$ −12.26 in the experiment of Fig. 2. (b) Fitting of the time course of $I$ according to Eq. (8) for a reversible first-order reaction, assuming the equilibrium intensity $I_e = 0.66$, corresponding to $K = 0.5$.

The intensity of the resonances of $H_a$ and $H_c$ remained notably constant in the time of the experiment (about 5 days) and no H transfer to other pyridinic carbon atoms was observed. The rate of the hydrogen transfer became progressively slower and an equilibrium was attained when about 1/3 of the H atoms had been transferred from $H_b$ to $H_\alpha$ (Fig. 3(a)). The decrease of the intensity of the resonance of $H_b$ could be nicely fitted as a reversible first-order process (Fig. 3(b)), with $k_{obs}$ for the direct step equal to $1.9(1) \times 10^{-6}$ s$^{-1}$.

These results are easily accounted for by an intramolecular sequence (Scheme 3) involving the reductive elimination of $H_b$ and of the metallated C atom from **2b**, to give the intermediate **I2'**, followed by the rotation of the terminally bound pyridine and the oxidative addition of the pyridinic ortho C–D bond, to give $[Re_3(\mu\text{-}H)(\mu\text{-}D)_2(\mu\text{-}NC_5D_3H)(CO)_{10}]^-$ (**2b'**). An analogous coordinatively unsaturated intermediate has been previously established for the reversible reductive elimination of benzene from the dinuclear complex

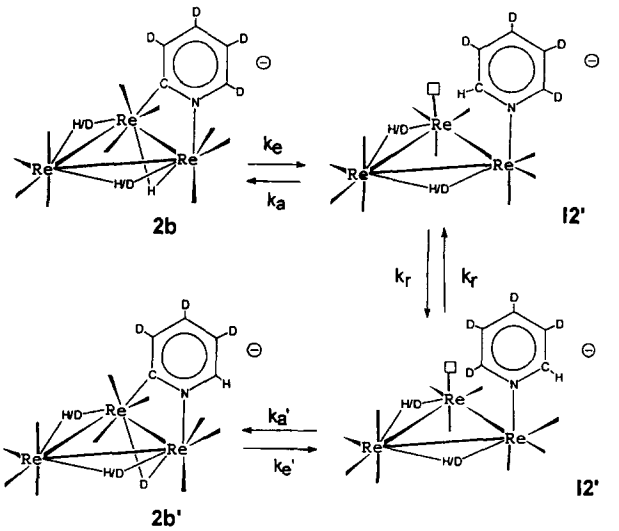


Scheme 3.

$[(\eta^5\text{-}C_5Me_5)(C_6H_5)Ir(\eta^1,\eta^3\text{-}C_3H_4)(\mu\text{-}H)Ir(\eta^5\text{-}C_5Me_5)]$ [8].

Examples of selective ortho-H/D exchanges have been reported, mainly in mononuclear phosphine complexes, even at catalytic levels [9]. In this case an additional selectivity is observed, concerning the involved hydridic site. The selective deuteration of the site $H_b$ implies two points:

(i) the reductive elimination is highly regioselective. Only the basal hydride (i.e. the one bridging the Re–Re interaction bridged by the pyridine) is eliminated, in spite of the presence of another hydride *cis*-coordinated to the metallated C atom.

(ii) The basal Re–Re interaction remains unbridged until the C–D oxidative addition occurs. Probably the lifetime of **I2′** is not long enough to allow the scrambling of its two hydrides on the three cluster edges [10].

The alternative hypothesis (i.e. elimination from a lateral edge and H migration from the basal edge) would lead to an increase of the H content in sites $H_a$ and $H_c$, unless an unusually high [11] kinetic isotope effect was postulated.

The prevalence of **2b** over **2b′** at equilibrium in acetone is a thermodynamic isotope effect, due to the fact that deuterons tend to accumulate in stronger bonds [12] and C–H interactions have force constants larger than Re–H–Re ones. It can be easily shown that this corresponds to the ratio between the kinetic isotope effects for the oxidative addition and the reverse reductive elimination of C–H (C–D). By using the steady state approximation for intermediate **I2′** and by assuming $k_r \gg k_a$, the result is $k_{obs} = k_e / (1 + k_a/k'_a)$ (where the kinetic constants refer to the steps shown in Scheme 3). Relatively small $k_H/k_D$ values (from 1 to 2) have been usually found for both C–H oxidative addition to and reductive elimination from transition metals in low oxidation states [6,11]. From the above value of $k_{obs}$ it therefore follows that $k_e$ should be close to $5 \times 10^{-6}$ $s^{-1}$, in deuterated acetone, at room temperature (ca. 293 K).

In the second experiment, a sample of $[Re_3(\mu\text{-}H)_3(\mu\text{-}NC_5H_4)(CO)_{10}]^-$ (**2a**, $NEt_4^+$ salt) was dissolved in py-$d_5$, the NMR tube was sealed and was kept at 302 K. Spectra acquired at different times showed three main features (Fig. 4): (i) the decrease of the intensities of the four resonances of ortho-metallated pyridine, all with the same first-order rate constant $k = 2.9(1) \times 10^{-5}$ $s^{-1}$; (ii) the increase of the three resonances of the free pyridine; (iii) the decrease of the three hydridic resonances, initially much faster for $H_a$ and $H_c$ than for $H_b$ ($k = 1.3(2) \times 10^{-5}$ $s^{-1}$ vs. $4.3(8) \times 10^{-6}$ $s^{-1}$ from a rough first-order fitting of the data concerning the first 7 h only).

The points (i) and (ii) are easily accounted for by the sequence 3, involving the exchange between free

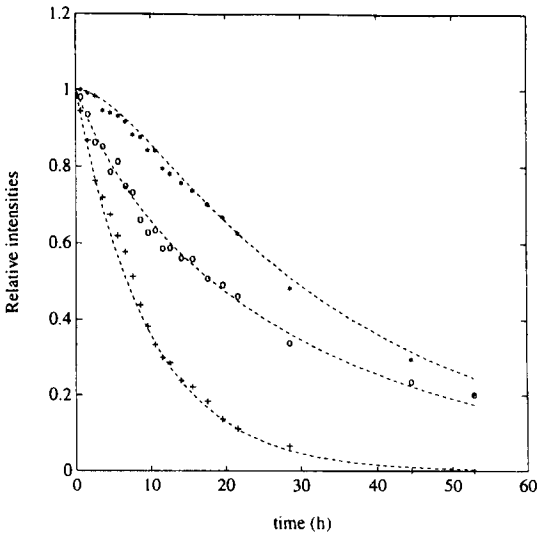


Fig 4. Time course of the intensities of selected protonic resonances of $[Re_3(\mu\text{-}H)_3(\mu\text{-}NC_5H_4)(CO)_{10}]^-$ (**2a**) in py-$d_5$ at 302 K: +, H–$C_\alpha$; *, $H_b$; o, $H_a$.

$(NC_5D_5)$ and coordinated $(NC_5H_5)$ pyridine in the $[Re_3H_2(CO)_{10}(Py)]^-$ intermediate formed by C–H reductive elimination.

$$[Re_3H_3(NC_5H_4)(CO)_{10}]^- \quad \textbf{2a}$$
$$\Leftrightarrow [Re_3H_2(CO)_{10}(NC_5H_5)]^- \quad \textbf{I2}$$
$$\rightarrow [Re_3H_2(CO)_{10}(NC_5D_5)]^- \quad \textbf{I2′}$$
$$\Leftrightarrow [Re_3H_2D(NC_5D_4)(CO)_{10}]^- \quad \textbf{2b} \qquad (3)$$

This sequence also implies the simultaneous H/D exchange for one hydride. The data of Fig. 4 indicate that this deuteration has a regioselectivity opposed to that observed in acetone, because the incoming D atom was initially located almost exclusively on the lateral edges of the triangle, as previously observed in the species **2b** obtained in the reaction of **1** with py-$d_5$. The initial rate of deuteration of these sites was in fact quite close to half the rate of pyridine elimination.

At longer times site $H_b$ also was involved in the H/D exchange and eventually a fully deuterated derivative was obtained. The intensities of the three resonances of the free pyridine grew at the same rate until the disappearance of **2a** was the dominant process, then only the ortho resonance increased selectively.

The fully deuterated species in pyridine-$H_5$ solution underwent the opposite D/H exchange and a $^1$H-NMR spectrum showed that, after one night, the intensities of the signals of $H_a$ and $H_c$ were higher than that of $H_b$. This further confirms the higher rate of exchange of the lateral edges of the triangle.

The opposite regioselectivity of the H/D exchange of the hydrides in py-$d_5$ and in acetone could have several origins. If the reductive elimination is an intramolecular process, the regioselectivity observed in acetone should be maintained in py-$d_5$. However, the intimate nature of the intermediate **I2** could be quite different in the two solvents, because of the possible coordination of pyridine on the vacant site [13]. The bis-pyridine species $[Re_3H_2(CO)_{10}(Py)_2]^-$ would just be the expected product of the reaction of **1** with pyridine according to Eq. (2), and an example has already been reported [14] showing the easy transformation of a bis-pyridine complex, [1,2-*eq*,*eq*-$Re_2(CO)_8(Py)_2$], into a cyclometallated derivative, $[Re_2(\mu\text{-}H)(\mu\text{-}NC_5H_4)(CO)_8]$. Owing to this stabilization by the solvent, the lifetime of the intermediate **I2** is therefore expected to be higher in pyridine than in acetone, thus allowing the scrambling of the hydrides on the triangle edges. Moreover, the coordination of two pyridines would also provide both steric and electronic reasons for the migration of one hydride on the basal (Py)Re–Re(Py) interaction. A lateral edge of the triangle would then become the site of coordination of H (or D) after the ortho-metallation. The fast process equalizing $H_a$ and $H_c$ would eventually lead to the even distribution of deuterium on these sites.

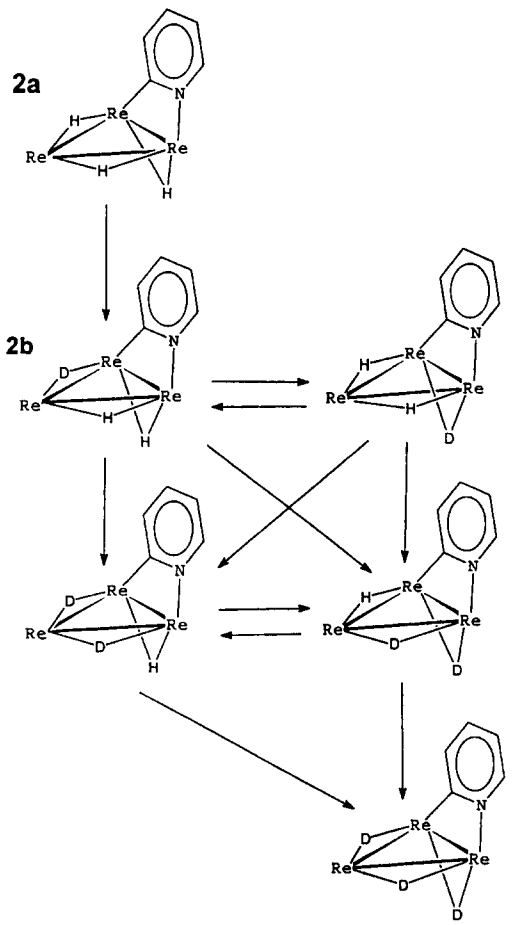


Scheme 4.

Alternatively, intermolecular mechanisms could be envisaged in pyridine solution. The reductive elimination and the coordination of the second pyridine molecule could occur in a concerted way. This would favour the elimination of $H_a$ instead of $H_b$, in order to maintain an H bridge in the (Py)Re–Re(Py) interaction. The involvement of the pyridine solvent in the transition state is also supported by the fact that the rate of elimination of the ortho-metallated pyridine (which cannot be higher than the rate of the reductive elimination) was significantly higher than the rate of reductive elimination estimated in acetone solution (at room temperature $1.2 \times 10^{-5}$ vs. ca. $5 \times 10^{-6}$ $s^{-1}$).

Deprotonation/protonation steps could also be postulated, due to the basicity of pyridine. Such processes, however, if occurring, should be confined into the solvation sphere, because no significant H transfer to water was observed in the course of these experiments. Moreover, no H/D exchange has been observed in py-$d_5$ for the hydrides of **3** below and there are no reasons to suppose a significantly higher acidity of the hydrides of the anion **2** than those of the anion **3**.

The stepwise deuteration of the hydridic sites of **2** most likely occurs therefore via consecutive metallation–demetallation cycles, like the sequence 3 described above. In each step, the incoming D atom is supposed to coordinate preferentially on a lateral edge. The deuteration of the $H_b$ site should therefore be the result of some H migration process. This is an integral part of the intramolecular hypothesis, whilst it should be an additional feature of the solvent-assisted pathway.

A general scheme for the stepwise deuteration of the three cluster edges is given in Scheme 4. According to the effective mechanism, some pathway could be negligible. Each vertical path implies an intermediate like **I2**, whilst no hypothesis is made about the mechanism of the horizontal pathway. The dotted lines reported in Figs. 1 and 4 have been obtained by taking into account only the vertical and horizontal pathways (no diagonal paths, intermolecular hypothesis), but alternative satisfactory fittings can be obtained by different choices. These fittings therefore do not have any specific mechanistic meaning, but only aim at showing that the experimental results can be simulated by models based on repeated cycles of reversible ortho-metallations.

Indeed, a rigourous kinetic treatment of the whole deuteration process could not be attempted, because too many possible processes (pyridine reductive elimination, oxidative addition, substitution, rotation, H migration, and relative isotopic effects) are involved to allow meaningful estimations of their relative rates.

As mentioned above, the measured rate of disappearance of the H atoms of ortho-metallated pyridine provides only a lower limit to the rate of the reductive

elimination, unless the pyridine substitution is fast with respect to the oxidative addition. The reaction of **2** with CO in py-$d_5$ (see below) has provided some kinetic evidence supporting this hypothesis.

### 2.2. Reaction of 2 with CO

In order to confirm the existence of the unsaturated, or solvent stabilized, intermediate **I2**, we tried to trap it by addition of a suitable ligand, such as CO.

When CO was bubbled in an acetone solution of **2**, at room temperature, a very slow reaction occurred ($t_{1/2} \approx 2$ days), leading to the formation of the cluster anion $[Re_3(\mu\text{-}H)_2(CO)_{12}]^-$, (**4**) [15], identified through its IR spectrum and its $^1$H-NMR resonance at $\delta$ −17.20.

$$[Re_3(\mu\text{-}H)_3(\mu\text{-}NC_5H_4)(CO)_{10}]^- + 2CO \rightarrow [Re_3(\mu\text{-}H)_2(CO)_{12}]^- + Py \quad (4)$$

Reaction 4 confirms that ortho-metallation can be reversed. Its rate agrees well with that of the reductive elimination step, estimated in the H/D exchange experiment in acetone (ca. $5 \times 10^{-6}$ s$^{-1}$).

The most likely pathway to **4** involves the intermediate formation of a $[Re_3(\mu\text{-}H)_2(CO)_{11}(Py)]^-$ anion, by addition of one CO ligand to the intermediate **I2**. NMR monitoring showed only one intermediate resonance ($\delta$ −13.56), with a very low intensity, roughly constant in the course of the experiment. The reaction was then repeated in pyridine, in order to reduce the rate of the pyridine substitution by CO (the initial dissociative step for substitution reactions in octahedral complexes being usually reversible). NMR monitoring, at room temperature, showed the slow transformation of **2** into a new species **3**, characterized by a resonance at $\delta$ −12.93 (in pyridine-$d_5$) and −13.56 in deuterated acetone. A single crystal X-ray analysis (see below) showed that **3** was indeed the expected $[Re_3(\mu\text{-}H)_2(CO)_{11}(Py)]^-$ intermediate.

$$[Re_3(\mu\text{-}H)_3(\mu\text{-}NC_5H_4)(CO)_{10}]^- + CO \rightarrow [Re_3(\mu\text{-}H)_2(CO)_{11}(Py)]^- \quad (5)$$

Kinetic measurements were performed at 302 K, in py-$d_5$ solution, in NMR tubes saturated with 1 atm of CO. The intensity of the resonances of the hydrogen atoms of the ortho-metallated pyridine in **2a** decreased according to a first-order rate constant $k = 3.0(1) \times 10^{-5}$ s$^{-1}$, i.e. with the same rate observed in the absence of CO, in the H/D exchange experiments. This suggests that the replacement of pyridine by py-$d_5$ (see Eq. (3)) is much faster than the successive reaction steps. In fact, if **I2** had a lifetime comparable to **I2′**, it could react with CO and then the rate of disappearance of **2a** would be affected by the presence of CO.

These data therefore support a mechanism implying the rate determining formation of the intermediate **I2**, its fast transformation into **I2′**, and then the competition between metallation and CO coordination.

Attempts were performed to estimate the competition ratio $r$ between the pseudo-first-order rate constant of the reaction of **I2′** with CO (assumed constant during the experiment) and the first-order constant for the intramolecular metallation. Two methods were employed, as detailed in the Experimental section, leading to $r = 0.45(15)$.

### 2.3. Reaction of 1 with CO in pyridine

The competition between C–H oxidative addition and CO coordination described above for intermediate **I2** should also occur in the course of the formation of the anion **2** from **1**, if the same intermediate **I2** is involved.

We therefore studied the reaction of the anion **1** in py-$d_5$ saturated with CO, at 302 K. It must be remarked that in "innocent" solvents such as acetone, **1** reacts with CO only under high pressures: at atmospheric pressure, no reaction was observed after 48 h, at room temperature [4]. In this case, in contrast, we observed the fast formation of both the anions **2** and **3**. At longer times **2** disappeared to give **3**, according to reaction 5. However, the profile of the concentration vs. time curves (Fig. 5) clearly showed that **3** did not originate from **2** only (according to a consecutive reaction path **1** → **2** → **3**) but also directly from **1**, through a parallel reaction. This is just what was expected on the basis of the presence of the intermediate **I2′** of Scheme 2, which leads to the kinetic scheme shown in Eq. (6) (see

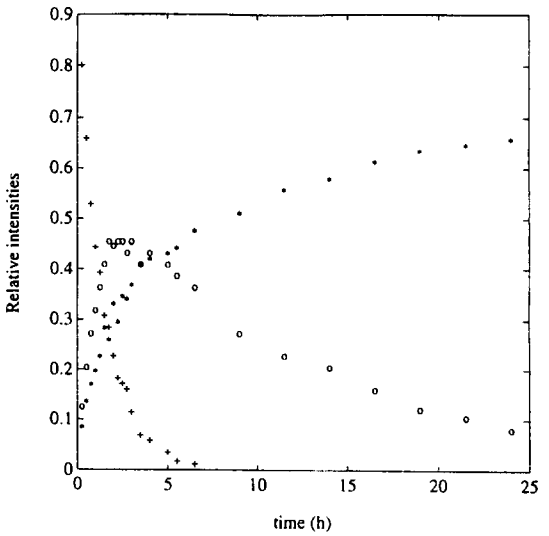


Fig. 5. Time course of the intensities of the hydridic resonances of **1** (+), **2b** ($H_b$, ○), **3** (*) during the reaction of **1** with CO in py-$d_5$ at 302 K. The low field resonance of **1** was used and, being due to 2 equivalent hydrides, was divided by 2, as was that of **3**.

Experimental section for the meaning of the kinetic symbols):

$$\mathbf{1} \xrightarrow{k_1} \mathbf{I2'} \underset{fk'_e}{\overset{k'_a}{\rightleftharpoons}} \mathbf{2b} \qquad (6)$$

$$\mathbf{I2'} \xrightarrow{k_c} \mathbf{3}$$

In a separate experiment we monitored the reaction of **1** in py-$d_5$, at the same temperature, to give the anion **2** only. The disappearance of **1** followed first-order kinetics in both the experiments, with the same rate constant ($k_1 = 2.1(2) \times 10^{-4}$ s$^{-1}$). This indicates that the intermediate leading to the anions **3** and **2** (**I2'**) is formed after the rate determining step. As to the nature of this step, there are no sound arguments to discriminate between the fast, reversible formation of an undetectable amount of **I1**, followed by slow $H_2$ elimination, or rather the rate determining addition of pyridine on **1** to give **I1**, which then rapidly undergoes $H_2$ elimination to give **I2'**.

A competition ratio $r = 0.5(1)$ was estimated, in excellent agreement with the value found for the reaction of **2** with CO, by using only the initial reaction data (up to 50% of conversion of **1**, in order to avoid the significant formation of highly deuterated isotopomers).

### 2.4. Reaction of 2 with $H_2$

The above results have shown the reversibility of the oxidative addition which is the last step of the pathway leading to **2** in Scheme 2. To verify the possible reversibility of the other steps of Scheme 2, according to reaction 7, we treated the anion **2** with $H_2$, in dichloromethane.

$$[Re_3(\mu\text{-}H)_3(\mu\text{-}NC_5H_4)(CO)_{10}]^- + H_2 \rightarrow [Re_3(\mu\text{-}H)_4(CO)_{10}]^- + Py \qquad (7)$$

A high hydrogen pressure had to be used in order for the reaction to proceed at a reasonable rate. Under 100 atm of $H_2$, the conversion to the anion **1** was ca. 15% after 15 h and ca. 75% after 6 days (at about 288 K). The selectivity of the transformation was satisfactory, because the NMR spectra of the reaction mixtures showed only few unattributed resonances, of very low intensity.

This result shows that the oxidative addition of $H_2$ can successfully compete with the intramolecular C–H oxidative addition, under high $H_2$ pressure. Moreover, it also shows that a H ligand is able to displace the pyridine ligand from the saturated species **I1** to give the

Table 1
Bond distances (Å) and angles (deg.) within $[Re_3(\mu\text{-}H)_2(CO)_{11}(Py)]^-$ (**3**)

| | | | |
|---|---|---|---|
| Distances | | | |
| Re(1)–Re(2) | 3.025(1) | Re(1)–C(13) | 2.02(3) |
| Re(1)–Re(3) | 3.202(1) | Re(1)–C(14) | 1.97(3) |
| Re(2)–Re(3) | 3.209(1) | Re(2)–C(21) | 1.88(2) |
| Re(1)–C(11) | 1.88(2) | Re(2)–C(22) | 1.91(3) |
| Re(1)–C(12) | 1.86(3) | Re(2)–C(23) | 1.91(3) |
| Re(2)–C(24) | 1.95(3) | N(1)–C(1) | 1.34(3) |
| Re(3)–C(31) | 1.88(3) | N(1)–C(5) | 1.36(3) |
| Re(3)–C(32) | 1.89(3) | C(1)–C(2) | 1.36(3) |
| Re(3)–C(33) | 1.87(3) | C(2)–C(3) | 1.36(3) |
| Re(3)–N(1) | 2.21(2) | C(3)–C(4) | 1.32(3) |
| | | C(4)–C(5) | 1.43(3) |
| Angles | | | |
| C(11)–Re(1)–C(12) | 94.2(10) | C(31)–Re(3)–N(1) | 88.1(9) |
| C(11)–Re(1)–C(13) | 93.0(9) | C(32)–Re(3)–N(1) | 89.6(10) |
| C(11)–Re(1)–C(14) | 90.2(10) | C(33)–Re(3)–N(1) | 174.8(9) |
| C(12)–Re(1)–C(13) | 87.0(10) | C(31)–Re(3)–Re(1) | 110.4(7) |
| C(12)–Re(1)–C(14) | 89.7(11) | C(32)–Re(3)–Re(1) | 160.1(9) |
| C(13)–Re(1)–C(14) | 175.6(10) | C(33)–Re(3)–Re(1) | 95.1(8) |
| C(11)–Re(1)–Re(2) | 173.6(6) | N(1)–Re(3)–Re(1) | 87.6(4) |
| C(12)–Re(1)–Re(2) | 91.9(7) | C(31)–Re(3)–Re(2) | 166.2(7) |
| C(13)–Re(1)–Re(2) | 85.3(7) | C(32)–Re(3)–Re(2) | 104.3(9) |
| C(14)–Re(1)–Re(2) | 91.8(7) | C(33)–Re(3)–Re(2) | 90.7(8) |
| C(21)–Re(2)–C(22) | 94.1(11) | N(1)–Re(3)–Re(2) | 94.5(5) |
| C(21)–Re(2)–C(23) | 90.9(10) | C(22)–Re(2)–Re(1) | 88.3(8) |
| C(21)–Re(2)–C(24) | 90.3(10) | C(23)–Re(2)–Re(1) | 91.8(7) |
| C(22)–Re(2)–C(23) | 92.6(11) | C(24)–Re(2)–Re(1) | 86.9(6) |
| C(22)–Re(2)–C(24) | 88.4(10) | C(31)–Re(3)–C(32) | 89.2(11) |
| C(23)–Re(2)–C(24) | 178.4(10) | C(31)–Re(3)–C(33) | 86.8(11) |
| C(21)–Re(2)–Re(1) | 176.3(8) | C(32)–Re(3)–C(33) | 89.4(11) |

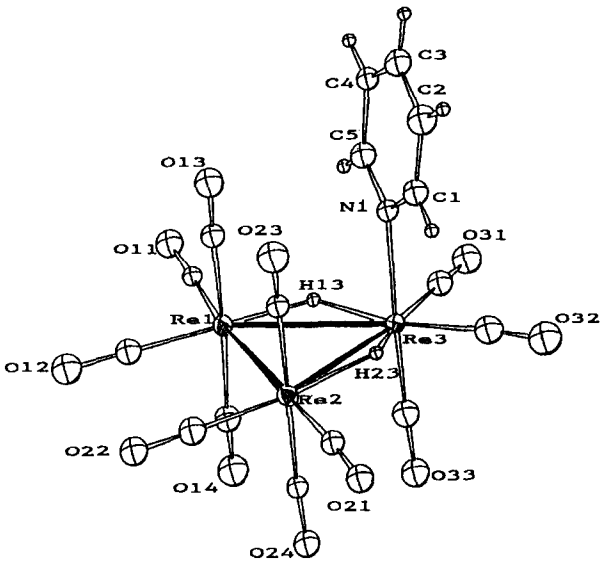


Fig. 6. A view of the anion $[Re_3(\mu\text{-}H)_2(CO)_{11}(Py)]^-$ (3). For clarity the numbering of the carbonyl groups is indicated only by the labels of their oxygen atoms.

unsaturated anion **1**. This confirms the peculiar stability of $Re(\mu\text{-}H)_2Re$ unsaturated systems in the chemistry of rhenium clusters. On the other hand, it has been previously shown that the anion **1** can be formed by substitution of two CO molecules by reaction with $H_2$, at high temperature and pressure [4].

### 2.5. Structure of $[Re_3(\mu\text{-}H)_2(CO)_{11}(Py)][NEt_4]$ (3)

The crystal structure consists of the packing of discrete $[Re_3(\mu\text{-}H)_2(CO)_{11}(Py)]^-$ anions and tetraethylammonium cations in the ratio 1:1, separated by normal van der Waals contacts. The anion is illustrated in Fig. 6 and bond distances and angles are given in Table 1. It displays an idealized $C_s$ symmetry, an approximate mirror plane passing through Re(3), the nitrogen atom of the pyridine molecule and the mid-point of the Re(1)–Re(2) edge. The metal atoms form an isosceles triangle, with one shorter and two longer edges, consisting of two $Re(CO)_4$ and one $Re(CO)_3(Py)$ units. The two longer edges are bridged by two hydrido ligands, which were located indirectly by non-bonding potential energy calculations.

The stereochemistry of the anion can in general be related to that of the family $[Re_3(\mu\text{-}H)_{3-n}(CO)_{12}]^{n-}$, and in particular to that of $[Re_3(\mu\text{-}H)_2(CO)_{12}]^-$ [15], by replacement of one axial CO group by a pyridine ligand. In these species axial substitution by two electron donor ligands (in a *trans* position to a CO group) is usually observed [16,17] instead of equatorial substitution (in a *trans* position to a hydride or to a metal–metal bond), and among the structurally characterized derivatives only $[Re_3(\mu\text{-}H)_3(CO)_{11}(PPh_3)]$ [18] belongs to the second class.

The Re–Re hydrogen-bridged edges display the expected lengthening with respect to the unbridged one [3.202(1) and 3.209(1) Å vs. 3.025(1) Å]. A comparison with the metal–metal bond lengths found in $[Re_3(\mu\text{-}H)_2(CO)_{12}]^-$ [3.173(7), 3.181(7) and 3.035(7) Å] [15] shows that the major difference consists in a moderate elongation of the longer edges, very probably due to the presence of the bulkier pyridine ligand.

The geometry about the rhenium atoms can be described as distorted octahedron, taking into account both the hydrido ligands and the direct Re(1)–Re(2) bond. The Re–C bond distances exhibit a normal pattern of values, those involving mutually *trans* carbonyl ligands being on average longer than the other ones.

The pyridine ligand is coordinated to Re(3) with a Re–N bond distance, 2.21(2) Å, which compares well with the similar interactions in $[Re_3(\mu\text{-}H)_3(CO)_{10}(Py)_2]$ (mean 2.22 Å) [17], $[Re_3(\mu\text{-}H)_4(CO)_9(Py)]^-$ [2.21(1) Å] [19] and $[Re_3(\mu\text{-}H)_3(\mu\text{-}NC_5H_4)(CO)_9(Py)]^-$ [2.236(7) Å] [3]. The plane of the aromatic ring is almost perpendicular to the plane of the metal triangle and, as in the above related clusters, it lies nearly parallel to the opposite edge Re(1)–Re(2), in order to minimize the non-bonding interactions with the other axial ligands. The dihedral angle between the plane of the aromatic ring and the plane C(13)–Re(1)–Re(2)–C(23) is 15(1)°.

Of the two possible isomers with the pyridine ligand in axial coordination the preferred one in the solid state is that with higher symmetry. From a steric point of view this can be explained bearing in mind that, in this geometry, the pyridine molecule presents longer non-bonding contacts with both the facing axial CO ligands.

The location of the hydrides as bridging the two equivalent Re–Re interactions found in the solid state is probably also maintained in solution, because of the presence of only one hydridic resonance in the NMR spectrum (even at −80 °C). This is consistent with the preference for hydride ligands to bridge the most electron rich metal–metal bonds. However, a fast scrambling of the hydrides on the three edges cannot be definitely ruled out, because such dynamic processes are quite easy in triangular clusters containing one unbridged M–M interaction.

### 2.6. Conclusions

It has been definitely ascertained that in solutions of the anion **2** the slow transfer of one hydride to the C atom of the ortho-metallated pyridine occurs, restoring a C–H bond. This occurs also in the absence of other added ligands and in solvents of low coordinating capability (such as acetone).

Both the rate and the regioselectivity of this transfer are affected by the nature of the solvent, indicating the

possible involvement in the rate determining step of the solvent itself, at least when it has a high coordinating capability. The presence of a ligand such as CO, however, does not affect the rate of the reductive elimination.

The reductive elimination is followed by a novel, fast C–H oxidative addition, which can lead to H/D exchange between the cluster and the organic molecule, if suitable isotopomers are used. An equilibrium isotopic effect showing the expected preference for C–D and Re–H–Re bonds with respect to C–H and Re–D–Re ones has been shown.

In the presence of CO, in pyridine solution, **2** transforms into the anion **3**, which contains the terminally bound pyridine formed in the reductive-elimination act. Kinetic measurements support a mechanism based on the competition between C–H oxidative addition and CO coordination in an 'unsaturated' (probably solvent stabilized) intermediate. The oxidative addition is kinetically favoured, its rate constant being about twice that for CO coordination (under 1 atm of CO).

The unsaturated anion **1**, which is inert toward CO at atmospheric pressure, reacts with it in pyridine solution. Kinetic measurements show that reaction process via pyridine coordination, followed by the same competition between CO coordination and ortho-metallation observed for the reaction of the anion **2** with CO.

In spite of the unfavourable competition ratio, the derivative of CO coordination is the only final product, owing to the irreversibility of the pathway leading to it. The effectiveness of CO as a catalyst poison could arise therefore more from thermodynamic than from kinetic factors.

The coordinatively unsaturated intermediate generated by the reductive elimination is also able to activate the $H_2$ molecule, even if a high $H_2$ pressure is necessary to effectively compete with the intramolecular ortho-metallation. This provides a further example [20,21] of a room temperature transformation of a saturated cluster into an electronically unsaturated one.

## 3. Experimental section

The reactions were performed under $N_2$ in solvents dried and deoxygenated by standard methods. $[NEt_4][Re_3(\mu\text{-}H)_4(CO)_{10}]$ [4] and $[NEt_4][Re_3(\mu\text{-}H)_3(\mu\text{-}NC_5H_4)(CO)_{10}]$ [3] were prepared by previously published methods. Pyridine was distilled over KOH just before the reaction. Acetone-$d_6$ and pyridine-$d_5$ (Merck) were used as received. IR spectra were recorded in 0.1 mm $CaF_2$ cells on a Perkin Elmer 781 grating spectrophotometer. The NMR spectra were obtained on Bruker WP80 and AC200 spectrometers; the temperature of the experiments was calibrated using the ethylene glycol/DMSO-$d_6$ standard solution and controlled by the spectrometer BVT 1000 unity.

### 3.1. NMR monitoring of the reaction processes

In a typical experiment 15 mg (ca. 0.015 mmol) of compound **1** or **2** were dissolved in the proper solvent in the NMR tubes, which were either sealed under vacuum or closed with a screw cap. When NMR tubes with standard stoppers were used, a significant increase of the water resonance was observed during the experiments, while in the sealed tubes such an increase became almost negligible. For the reaction with CO, the py-$d_5$ solvent was equilibrated with CO at room temperature for 30 min before introducing the reagent. The NMR tubes were then placed in the instrumental probe and spectra were recorded at different times. When needed, the tubes were placed in a thermostatic bath (Haake F3) in the intervals between spectra.

The integrated intensity of the $NCH_2$ cationic signal was used as internal standard in order to normalize the integrated intensities of the resonances of interest in each spectrum.

The relaxation times of the protonic resonances of the mixture of $[Re_3(\mu\text{-}H)_2(\mu\text{-}D)(\mu\text{-}NC_5D_4)(CO)_{10}]^-$ (**2b**) and $[Re_3(\mu\text{-}H)(\mu\text{-}D)_2(\mu\text{-}NC_5D_3H)(CO)_{10}]^-$ (**2b'**) in acetone-$d_6$ were measured by a standard non-selective inversion recovery pulse sequence and were 6.6 ($H_\alpha$), 1.7 ($H_b$), 1.5 ($H_c$) and 1.6 ($H_a$) s. The relaxation times of both free pyridine-$H_5$ and free pyridine-$HD_4$ in py-$d_5$ were about 60–70 s. To ensure reliable integration ratios of the pyridine hydrogens, a relaxation delay of 90 s was used between each pulse (75° pulse) in the spectra in py-$d_5$.

### 3.2. Kinetic treatment of the data

#### 3.2.1. H / D exchange in acetone

The intensity $I$ of the hydridic resonance of **2b** at $\delta$ −12.25 was used as a probe of the concentration of this isotopomer and the kinetic constant for the forward reaction **2b** → **2b'** was estimated by least-squares fitting of Eq. (8), describing the approach toward equilibrium for reversible first-order reactions (Fig. 3(b)), where $I_e$ represents the intensity at the equilibrium (assumed as 0.66, corresponding to an equilibrium constant $K$ = **2b'**/**2b** = 0.5).

$$[K/(1+K)]\,ln[(I-I_e)/(I-I_e)] = kt \qquad (8)$$

#### 3.2.2. H / D exchange in py-$d_5$

Each vertical step of the general Scheme 4 was detailed as shown in the Eqs. (3) and (9) for the **2a** → **2b** step.

$$\mathbf{2a} \underset{k_a}{\overset{k_e}{\rightleftharpoons}} \mathbf{I2} \xrightarrow{k_s} \mathbf{I2'} \underset{fk'_e}{\overset{k'_a}{\rightleftharpoons}} \mathbf{2b} \qquad (9)$$

The kinetic equations were obtained by applying the steady state approximation to intermediates **I2** and **I2'**, and by assuming $k_s \gg k_a$. Therefore these constants did not appear in the final equations and $k_e$ was set equal to the value estimated from the least-square first-order fit of the decrease of the intensity of the resonances of the ortho-metallated pyridine. The rate constant $k'_e$ differs from $k_e$ due to isotope effects, and $f$ is a statistical factor accounting for the probability that the elimination involves D rather than H. In the hypothesis that the elimination concerns the hydrides on the lateral edges, $f$ would be 0.5. Proper statistical corrections were also applied to the constants of the other steps of the Scheme 4, including the constants $k_i$ describing the interconversions between isotopomers containing the same number of D atoms (horizontal paths). The solution of the system of differential equations, for a given kinetic model and a given set of kinetic constants, was performed by a Runge–Kutta method (routine ODEC23 of the program MATLAB). This provided the time course of the concentration of the different isotopomers, and therefore of the selected NMR resonances. The fits reported in Figs. 1 and 4 were obtained by using a model without diagonal pathways and by assuming $k'_e = 0.5\ k_e$, and $k_i = k_e$. The success of the last assumption suggests that the horizontal isomerizations also occur via rate determining reductive eliminations.

### 3.2.3. Reaction of 2 with CO in py-$d_5$

The kinetic scheme described above was used and the competition for the coordination of CO on intermediate **I2'** was added, with a pseudo-first-order constant $k_c$. The concentration of CO in solution in fact can be assumed as nearly constant during the reaction, because the moles of CO contained in a screw cap NMR tube at atmospheric pressure and room temperature are about one order of magnitude higher than the moles of the reagent. In this way, the rate of formation of the isotopomer **3a** (all protium) was $[r/(1+r)][k_e\mathbf{2a} + k'_e\mathbf{2b}]$, where $r$ indicates the competition ratio $k_c/k'_a$. The value of $r$ that allows the best fit of the experimental data was then sought, by applying the same models and the same kinetic constants used to fit the H/D exchange to the initial reaction data only (when the only deuterated isotopomer is **2b**). Values of 0.35 and 0.55 were obtained in two different experiments, the scattering of the data probably being due to the difficulty in ensuring reproducible CO concentration. In a second approach to estimate $r$, the pathways leading to **2b** and **3a** from **2a** have been treated as parallel reactions and a plot of **3a** vs. **2a** for the initial reaction times (where the presence of other isotopomers and the pathway to **3a** from **2b** can be left out of account) resulted a straight line, whose slope provided the ratio $k_c/(k_c + k'_a)$ of 0.25 and 0.34 in the two different experiments, corresponding to $r =$ 0.33 and 0.52, respectively.

### 3.2.4. Reaction of 1 with CO in py-$d_5$

The above kinetic scheme was used, by substituting **2a** with **1** and introducing the rate constant $k_1$ (whose value was provided by least-squares first-order fits of the disappearance of **1**) to account for the formation of **I2'**. The value of $r$ was estimated as described above.

### 3.3. Isolation and spectroscopic characterization of [$NEt_4$]3

A 30 mg sample of $[NEt_4][Re_3(\mu\text{-}H)_3(\mu\text{-}NC_5H_4)(CO)_{10}]$, dissolved in 5 ml of pyridine saturated with CO, was stirred at room temperature for 3 days. The solution was evaporated to dryness and the residue dissolved in dichlomethane. Slow diffusion of diethyl ether produced cream crystals suitable for X-ray diffraction. IR ($\nu$ CO, acetone) 2062w, 2010s, 1958s, 1903m $cm^{-1}$. NMR ($\delta$, acetone-$d_6$) 8.6 (m, 2), 7.7 (m, 1), 7.4 (m, 2), −13.56 (2).

### 3.4. Reaction of [$NEt_4$]2 with $H_2$

A tube containing 10 mg (ca. 0.01 mmol) of $[NEt_4][Re_3(\mu\text{-}H)_3(\mu\text{-}NC_5H_4)(CO)_{10}]$, dissolved in

Table 2
Crystal data and intensity collection parameters for $[Re_3(\mu\text{-}H)_2(CO)_{11}(Py)][NEt_4]$ (**3**)

| | |
|---|---|
| Formula | $C_{24}H_{27}N_2O_{11}Re_3$ |
| Formula weight | 1078.08 |
| Crystal system | Monoclinic |
| Space group | $P2_1/c$ (no. 14) |
| $a$ (Å) | 14.327(3) |
| $b$ (Å) | 12.310(2) |
| $c$ (Å) | 17.437(3) |
| $\beta$ (deg) | 91.67(2) |
| $V$ (Å$^3$) | 3074.0(10) |
| $Z$ | 4 |
| $F$(000) | 1992 |
| $D$ (calc) (g $cm^{-3}$) | 2.329 |
| Temperature (K) | 293(2) |
| Diffractometer | CAD4 |
| Radiation (graph monochr) (Å) | 0.71073 |
| Absorption coefficient ($mm^{-1}$) | 11.840 |
| Crystal size (mm) | 0.25×0.17×0.15 |
| Scan method | $\omega$ |
| Scan interval (deg) | 1.1 + 0.35tg($\theta$) |
| Max time per reflection (s) | 70 |
| $\theta$ range (deg) | 3 to 24 |
| Reflections collected | 4823 |
| Independent reflections | 4823 [$R$(int) = 0.0000] |
| Crystal decay (%) | 8 |
| Absorption correction | $\psi$-scan |
| No. azimuth reflections | 3 |
| Min. transmission | 0.667 |
| Ref. least-sq. method | Full-matrix on $F_o^2$ |
| Obs reflection criterion | $> 2\sigma(I)$ |
| Data/restraints/parameters | 2064/0/176 |
| Goodness-of-fit on $F_o^2$ | 1.069 |
| Final $R$ indices [$I > 2\sigma I$] | $R1$ 0.0397, w$R^2$ 0.0835 |

Weighting calc $w = 1/[\sigma^2(F_o^2) + (0.0322P)^2 + 59.5766P]$ where $P = (F_o^2 + 2F_c^2)/3$

dichloromethane, was introduced into an autoclave under 100 atm of $H_2$, at room temperature (about 288 K). After 15 h, the solution was evaporated to dryness and the residue was analyzed by NMR, in deuteroacetone. The solution was again evaporated to dryness, and the residue, dissolved in dichloromethane, was transferred to the autoclave for 6 days, in the same conditions as above.

### 3.5. X-ray analysis of $[NEt_4][Re_3(\mu\text{-}H)_2(CO)_{11}(Py)]$

#### 3.5.1. Intensity measurements

Crystal data are reported in Table 2. The crystal sample was mounted on a glass fibre in the air. The intensity data were collected on an Enraf-Nonius CAD4 automated diffractometer at room temperature, using graphite monochromatized Mo K$\alpha$ radiation. The setting angles of 25 random intense reflections [$16° < 2\theta < 25°$] were used to determine by least-squares fit accurate cell constants and the orientation matrix. The collection was performed by the $\omega$-scan method, within the limits $6° < 2\theta < 48°$. A variable scan-speed and a variable scan-range were used, with a 25% extension at each end of the scan-range for background determination. Three standard intense reflections, monitored every 3 h, showed a crystal decay upon X-ray exposure, of ca. 8% at the end of the collection. The intensities were corrected for Lorentz, polarization and decay effects. An empirical absorption correction was applied to the data, based on $\psi$-scans ($\psi$ 0–360 every 10°) of three

Table 3
Atomic coordinates and equivalent isotropic displacement parameters (Å$^2$) for **3**: $U$(eq) is defined as one third of the trace of the orthogonalized $U_{ij}$ tensor

| | $x$ | $y$ | $z$ | $U$ (eq) |
|---|---|---|---|---|
| Re(1) | 0.14987(6) | 0.26108(9) | 0.04818(5) | 0.0468(3) |
| Re(2) | 0.23061(6) | 0.15117(9) | −0.09019(5) | 0.0479(3) |
| Re(3) | 0.36342(6) | 0.30895(8) | 0.01080(5) | 0.0434(3) |
| C(11) | 0.1135(13) | 0.331(2) | 0.1383(11) | 0.041(5) |
| O(11) | 0.0873(12) | 0.370(2) | 0.1955(9) | 0.075(5) |
| C(12) | 0.032(2) | 0.201(2) | 0.0275(13) | 0.064(7) |
| O(12) | −0.0438(14) | 0.164(2) | 0.0156(10) | 0.093(6) |
| C(13) | 0.182(2) | 0.122(2) | 0.1040(13) | 0.059(7) |
| O(13) | 0.2021(12) | 0.046(2) | 0.1362(10) | 0.083(6) |
| C(14) | 0.114(2) | 0.390(2) | −0.0124(14) | 0.068(8) |
| O(14) | 0.0939(13) | 0.465(2) | −0.0453(11) | 0.094(6) |
| C(21) | 0.285(2) | 0.091(2) | −0.1775(13) | 0.059(7) |
| O(21) | 0.3165(11) | 0.064(2) | −0.2359(10) | 0.074(5) |
| C(22) | 0.108(2) | 0.100(2) | −0.1165(14) | 0.073(8) |
| O(22) | 0.0352(12) | 0.061(2) | −0.1332(9) | 0.079(5) |
| C(23) | 0.261(2) | 0.024(2) | −0.0323(13) | 0.058(7) |
| O(23) | 0.2800(14) | −0.060(2) | −0.0028(12) | 0.108(7) |
| C(24) | 0.201(2) | 0.284(2) | −0.1469(13) | 0.054(6) |
| O(24) | 0.1861(11) | 0.361(2) | −0.1852(9) | 0.071(5) |
| C(31) | 0.414(2) | 0.413(2) | 0.0790(14) | 0.064(7) |
| O(31) | 0.4458(13) | 0.480(2) | 0.1204(11) | 0.091(6) |
| C(32) | 0.482(2) | 0.294(3) | −0.033(2) | 0.085(9) |
| O(32) | 0.554(2) | 0.284(2) | −0.0622(12) | 0.110(7) |
| C(33) | 0.337(2) | 0.424(2) | −0.0558(14) | 0.068(7) |
| O(33) | 0.3226(12) | 0.500(2) | −0.0947(10) | 0.081(5) |
| N(1) | 0.4023(12) | 0.183(2) | 0.0958(9) | 0.050(5) |
| C(1) | 0.455(2) | 0.097(2) | 0.0783(14) | 0.064(7) |
| C(2) | 0.492(2) | 0.027(3) | 0.132(2) | 0.082(9) |
| C(3) | 0.475(2) | 0.042(2) | 0.207(2) | 0.071(8) |
| C(4) | 0.420(2) | 0.123(2) | 0.2277(12) | 0.052(6) |
| C(5) | 0.383(2) | 0.195(2) | 0.1710(13) | 0.067(7) |
| N(1S) | 0.1904(13) | 0.729(2) | 0.2195(10) | 0.058(5) |
| C(1S) | 0.187(2) | 0.761(3) | 0.138(2) | 0.106(10) |
| C(2S) | 0.137(2) | 0.631(3) | 0.243(2) | 0.086(9) |
| C(3S) | 0.290(2) | 0.707(3) | 0.247(2) | 0.117(12) |
| C(4S) | 0.155(2) | 0.829(3) | 0.260(2) | 0.090(9) |
| C(5S) | 0.213(2) | 0.658(3) | 0.085(2) | 0.132(13) |
| C(6S) | 0.032(2) | 0.633(3) | 0.217(2) | 0.114(11) |
| C(7S) | 0.356(2) | 0.799(3) | 0.242(2) | 0.131(13) |
| C(8S) | 0.155(2) | 0.817(3) | 0.345(2) | 0.117(11) |

suitable reflections with $\chi$ values close to 90°. A set of 2064 significant [$I > 2\sigma(I)$] independent reflections was used in the structure solution and refinement.

*3.5.2. Structure solution and refinements*

All the computations were performed on a Silicon Graphics Indigo computer running IRIX 4.01, using the SHELXL-93 programs [22] and the physical constants tabulated therein.

The structure was solved by Patterson and Fourier methods, which revealed the locations of all the non-hydrogen atoms. The refinements were carried out by full-matrix least-squares against $F_o^2$. Anisotropic thermal parameters were assigned to the metal atoms only. Anisotropic refinement of the other non-hydrogen atoms was rejected because it resulted in a non-realistic ellipsoid for one C atom and gave an insignificant lowering of the agreement indices. The hydrogen atoms of the aromatic ring and of the cation were located in ideal positions (C–H 0.95 Å, riding refinement). Since no direct evidence was obtained from the difference Fourier maps, the hydrido ligands were located using Orpen's HYDEX program [23], assuming Re–H interactions of 1.85 Å. They were also included in the structure factor calculations ($U = 0.10$ Å$^2$) but not refined. The final difference-Fourier map was flat, showing only some residual peaks not exceeding ca. 1.0 e Å$^{-3}$. The final positional parameters are given in Table 3.

*Supplementary material available*

The supplementary material includes a complete table of bond distances and angles, anisotropic thermal factors, the calculated fractional coordinates of the hydrogen atoms, and a list of observed and calculated structure factor moduli.

## Acknowledgement

Special thanks are due to Mr Pasquale Illiano for the careful acquisition and integration of a countless number of NMR spectra.

## References and notes

[1] See for instance E.L. Muetterties, *Bull. Soc. Chim. Belg., 84* (1975) 959.
[2] See for instance, G. Lavigne and H.D. Kaesz, in B.G. Gates, L. Guczi and H. Knözinger (eds.), *Metal Clusters in Catalysis*, Elsevier, 1986, Ch. 4, p. 43, and Refs. therein.
[3] T. Beringhelli, G. D'Alfonso, G. Ciani, D.M. Proserpio and A. Sironi, *Organometallics, 12* (1993) 4863.
[4] T. Beringhelli, G. Ciani, G. D'Alfonso, H. Molinari and A. Sironi, *Inorg. Chem., 24* (1985) 2666.
[5] T. Beringhelli, G. Ciani, G. D'Alfonso and M. Freni, *J. Organomet. Chem., 311* (1986) C51.
[6] A.D. Ryabov, *Chem. Rev., 90* (1990) 403.
[7] The previous statement [3] ruling out "significant H/D exchange at room temperature and in the reaction time" is still substantially correct, because the difference between the rate of deuteration and that of formation of **2** is of one order of magnitude.
[8] W.D. McGhee, F.J. Hollander and R.G. Bergman, *J. Am. Chem. Soc., 110* (1988) 8428.
[9] See for instance M.I. Bruce, *Angew. Chem. Int. Ed. Engl., 16* (1977) 73 and Refs. therein.
[10] An agostic interaction could also be postulated, as suggested by one of the referees.
[11] E. Rosenberg, *Polyhedron, 8* (1989) 383 and Refs. therein.
[12] H.U. Siehl, *Adv. Phys. Org. Chem., 23* (1987) 63.
[13] The coordination of a second pyridine molecule also provides a possible pathway for the substitution of pyridine in Eq. (3).
[14] D.R. Gard and T.L. Brown, *Organometallics, 1* (1982) 1143.
[15] M.R. Churchill, P.H. Bird, H.D. Kaesz, R. Bau and B. Fontal, *J. Am. Chem. Soc., 90* (1968) 7135.
[16] T. Beringhelli, G. D'Alfonso, M. Freni, G. Ciani, M. Moret and A. Sironi, *J. Chem. Soc. Dalton Trans.* (1989) 1143 and Refs. therein.
[17] G. Ciani, G. D'Alfonso, M. Freni, P. Romiti and A. Sironi, *J. Organomet. Chem., 186* (1980) 353.
[18] C. Y Wei, L. Garlaschelli, R. Bau and T.F. Koetzle, *J. Organomet. Chem., 213* (1981) 63.
[19] T. Beringhelli, G. D'Alfonso, M. Freni, G. Ciani, A. Sironi and H. Molinari, *J. Chem. Soc. Dalton Trans.* (1986) 2691.
[20] T. Beringhelli, G. D'Alfonso, A.P. Minoja, G. Ciani and D.M. Proserpio, *Inorg. Chem., 32* (1993) 803.
[21] T. Beringhelli and G. D'Alfonso, *J. Chem. Soc. Chem. Commun.* (1994) 2631.
[22] G.M. Sheldrik, *SHELXL-93: program for structure refinement*, University of Göttingen, Germany, 1994.
[23] A.G. Orpen, *J. Chem. Soc. Dalton Trans.* (1980) 2509.